

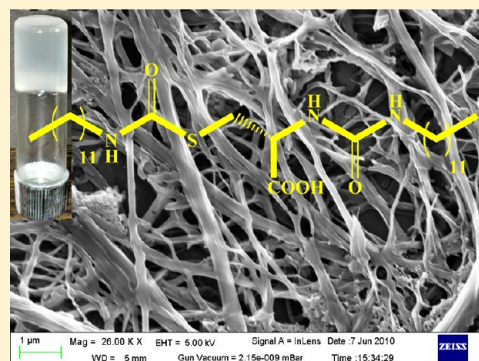
L-Cysteine-Derived Ambidextrous Gelators of Aromatic Solvents and Ethanol/Water Mixtures

Amrita Pal and Joykrishna Dey*

Department of Chemistry, Indian Institute of Technology, Kharagpur, Kharagpur-721 302, India

Supporting Information

ABSTRACT: A series of L-cysteine-derived double hydrocarbon chain amphiphilic gelators L-(3-alkyl-carbamoylsulfanyl)-2-(3-alkylurido)propionic acid with different hydrocarbon chain lengths (C6–C16) was designed and synthesized. These gelators efficiently gelate only aromatic solvents. The gelation ability increased with the increase of chain length up to C14, but then it dropped with further increase of chain length. The C12 and C14 derivatives also gelled ethanol/water mixtures. The gels were characterized by a number of methods, including FT-IR, NMR, and XRD spectroscopy, electron microscopy, and rheology. The amphiphiles were observed to form either flat lamellar or ribbonlike aggregates in aromatic solvents as well as in ethanol/water mixtures. The gelation in all the solvents employed was observed to be thermoreversible. The gel-to-sol transition temperature as well as mechanical strength of the organogels were observed to increase with the hydrocarbon chain length. Both types of gels of C8–C16 amphiphiles have gel-to-sol transition temperatures above the physiological temperature (310 K). FT-IR and variable temperature ^1H NMR measurements suggested that van der Waals interactions have major contribution in the gelation process. The gel-to-sol transition temperature and mechanical strength of the organogels in ethanol/water mixtures was observed to be higher than those of benzene organogel.



INTRODUCTION

Molecular gels (MGs) of low-molecular-weight gelators (LMWGs) in biofriendly solvents have attracted tremendous attention in the recent literature because of their potential applications in the pharmaceutical industry as soft materials for drug delivery and tissue engineering.^{1–3} Various LMWGs capable of forming gels in organic liquids and water^{1–21} have been reported in the literature. Many of these LMWGs are derivatives of sugars, amino acids, nucleotides, and peptides. The demand for better and environmentally friendly gelators makes amino-acid-based amphiphiles very attractive, as these compounds are usually biodegradable and biocompatible. In the past, several research works have explored the gelation by gelators containing amide linkage between the hydrophobic tail and the polar headgroup.^{22–28} In LMWGs containing amide groups (e.g., peptide-based systems), one of the interactions responsible for their supramolecular assembly is hydrogen bonding (H-bonding).^{29,30} Although some N-acyl amino acid derivatives containing a single amide group are known to gelate a number of hydrocarbon solvents, they cannot always supply abundant H-bonding that might be required in other liquids. Urea linkage has two hydrogen bond donor sites and one hydrogen bond acceptor site and is thus expected to act as a better H-bonding building block for supramolecular organization. There are many reports of LMWGs incorporating one or more urea functional groups in order to drive H-bond mediated assembly.^{27–30} In fact, urea function can form stronger hydrogen bonds than amide linkage,^{31–34} and one of

the lowest-mass organogelators reported in the literature is *N,N'*-dimethylurea.^{35–40} Hamilton and co-workers have reported that methyl and ethyl esters of *N*-(*n*-alkylcarbamoyl)-L-serine amphiphiles gel water above a critical concentration.²⁴ Recently, our group has demonstrated water-induced gelation of a range of organic solvents by amino acid-derived amphiphiles that contain urea function.⁴¹ The urea linkages can also act as receptors for anions, and this property has proven useful in the development of stimuli-responsive gels.^{42,43}

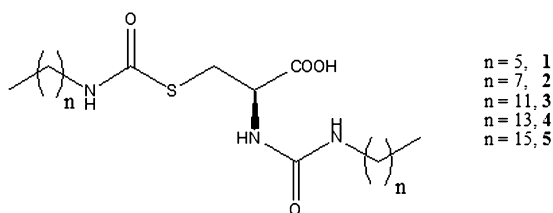
L-Cysteine is an important amino acid. It is found that S-allyl cysteine inhibits damage caused by oxidative stress in bovine endothelial cells and also inhibits oxidation of low-density lipoprotein at an optimum concentration of 1 mM.⁴⁴ Menger and co-workers have reported that *N*-benzoyl cysteine derivatives efficiently form hydrogels.⁴⁵ A cationic gemini surfactant based on L-cystine has also been shown to form thermoreversible hydrogel.⁴⁶ The gelation of aqueous L-cysteine/AgNO₃ system in the presence of different electrolytes has also been reported.⁴⁷ However, gelation behavior of L-cysteine-derived amphiphilic gelators have not been reported so far. Considering these facts, a series of new L-cysteine-derived amphiphiles, L-3-alkyl-carbamoylsulfanyl-2-(3-alkylurido)-propionic acid (see Chart 1 for structures) were designed and synthesized. The major objective of this study was to

Received: October 29, 2012

Revised: January 9, 2013

Published: January 22, 2013

Chart 1. Chemical Structure of the Amphiphiles



investigate the interactions responsible for gelation process. Unlike single chain amphiphiles, the molecules 1–5 have two hydrocarbon tails linked to the L-cysteine head through urea (NH–CO–NH) and carbamoylsulfanyl (NH–CO–S) linkages and therefore are capable of H-bonding, either between chains or between two molecules. Also there can be stronger intermolecular van der Waals interactions between hydrocarbon chains. Thus, gelation behavior of the amphiphiles in pure organic solvents as well as in ethanol/water mixtures is presented. We show here that while H-bonding is more important in gelation of organic solvents, van der Waals forces play a major role in polar or aqueous organic solvents. The organogels were characterized by a number of techniques, including ^1H NMR and FT-IR spectroscopy, field emission scanning electron microscopy (FESEM), X-ray diffraction (XRD), and rheology.

EXPERIMENTAL SECTION

Materials. The reagents L-cysteine, hexyl isocyanate, octyl isocyanate, dodecyl isocyanate, tetradecyl isocyanate, and hexadecyl isocyanate were obtained from Sigma-Aldrich (Bangalore, India) and were used as received. Triethylamine (TEA) was obtained from Merck, and it was dried and distilled before use. All solvents were locally procured in pure form and were directly used from the bottle. The gelators were synthesized following procedure reported in the literature.⁴¹ The details of synthesis and chemical identification of structures by ^1H NMR, ^{13}C NMR, and FT-IR spectra (Figures S1–S6) are included in the Supporting Information (SI).

Methods. Instruments. An AVANCE DAX-400 (Bruker, Sweden) 400 MHz NMR spectrometer was used to record NMR spectra of the compounds in CD_3OD solvent. The FT-IR spectra were measured with a Perkin-Elmer (model Spectrum Rx I) spectrometer. The melting point of solid compounds was measured with an Instind (Kolkata) melting point apparatus using open capillaries.

In a typical gelation test, 10 mg of gelator was weighed into a 4 mL screw-capped vial (8 mm o.d.), and organic solvent was added and then heated in a hot water bath to completely dissolve the solid. The resulting dispersion was then kept in a temperature controlled water bath at 298 K for cooling; gelation was confirmed when the material did not flow upon inversion of the vial. The gelation was observed in less than 30 min. The heating–cooling cycle was repeated for every addition of solvent. The critical gelation concentration (CGC) was determined from the maximum volume of solvent taken by a known mass of the gelator. The gel-to-sol transition temperature was determined by placing the screw-capped glass vials containing gels in a temperature-controlled water bath (Julabo model F12) and visually observing the flow upon tilt for every degree rise in temperature.

Electron micrographs were measured with a field emission scanning electron microscope (FESEM, Zeiss, Supra-40) operating at 5–10 kV. The specimens were prepared by placing the hot sample solution on the aluminum or copper foil, allowed to cool at room temperature, and then dried in desiccators for 24 h. A layer of gold was sputtered on top to make a conducting surface, and finally the specimen was transferred to the microscope.

The XRD measurements were performed at room temperature on a Pan Analytica X'Pert Pro X-ray diffractometer using Cu target (Cu $K\alpha$) and Ni filter at a scanning rate of 0.001 s^{-1} between 2° and 20° ,

operating at a voltage of 40 kV and current of 30 mA. The air-dried gel samples prepared on a glass slide were used.

Rheology measurements were performed on a Bohlin RS D-100 (Malvern, U.K.) rheometer using parallel-plate (PP-20) geometry. The gap between the plates was fixed at $100\ \mu\text{m}$. The gel samples were placed on the rheometer, and a stress-amplitude sweep experiment was performed at a constant oscillation frequency of 1.0 Hz at 25°C . The frequency sweep experiments were done using a fixed frequency of 10 Pa.

RESULTS AND DISCUSSION

Gelation of Organic Solvents. The gelation behavior of the amphiphiles was tested in a range of common aliphatic as

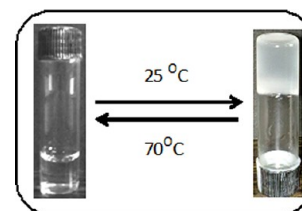


Figure 1. Sol–gel transition upon heating and cooling of the benzene gel of 4.

Table 1. Critical Gelation Concentration (CGC % w/v) of the Amphiphiles in Different Organic Solvents at 298 K (P = precipitate)

solvent	CGC (% w/v)				
	1	2	3	4	5
chloroform	P	P	P	P	P
benzene	5.1	3.1	2.0	0.9	1.4
toluene	5.9	3.7	2.5	1.4	2.1
<i>o</i> -xylene	5.2	3.4	2.2	1.0	1.5
<i>m</i> -xylene	5.5	3.5	2.5	1.3	1.9
<i>p</i> -xylene	5.3	3.9	2.8	1.7	2.3
mesitylene	5.8	3.6	2.4	1.2	1.8
chlorobenzene	5.6	3.3	2.1	1.0	1.6
nitrobenzene	5.5	3.4	2.3	1.2	1.9

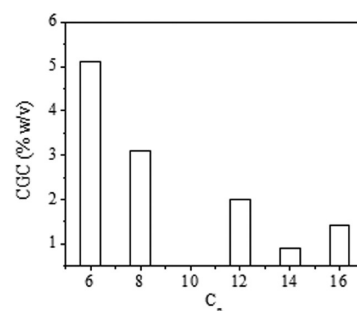


Figure 2. Variation of the CGC values of the benzene gel of amphiphiles having different hydrocarbon chain length.

well as aromatic organic solvents, including hexane, cyclohexane, heptane, benzene, toluene, *o*-, *m*-, and *p*-xylene, mesitylene, chlorobenzene, nitrobenzene, chloroform, and tetrachloromethane. However, the amphiphiles were found to gel only aromatic solvents above a certain concentration, called the CGC. The gelation was confirmed by the stability upon inversion of the screw-capped glass vial (Figure 1). These organogels also experience a gel-to-sol transition upon heating. The organogels thus formed at room temperature ($\sim 298\text{ K}$)

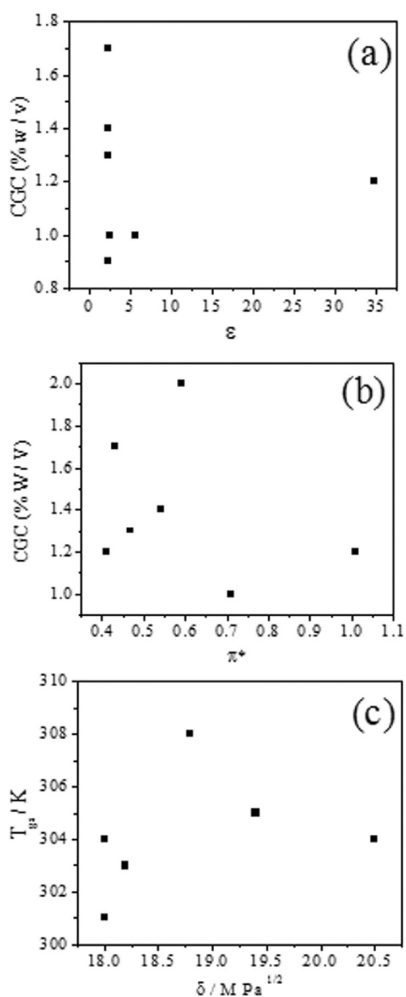


Figure 3. Variation of CGC of **4** in different solvents with (a) dielectric constant (ϵ), (b) Kamlet–Taft parameter (π^*) of the solvents, and (c) variation of T_g values of the organogel **4** at CGC with the solubility parameter (δ) of the solvents.

were visually opaque in all the solvents employed, except nitrobenzene in which the gel appeared to be translucent. The opacity of the organogels is associated with (i) the cross-sectional thickness of the crystalline aggregates, (ii) the number of junction zones capable of diffracting light, and (iii) the number of crystalline aggregates within the SAFiN. Since the organogels were observed to form after every heating–cooling cycle, the gelation is thermoreversible.

The gelation behavior of the amphiphiles in different pure solvents are summarized in Table 1. CGC was measured to compare gelation abilities of the amphiphiles. The results are included in Table 1. The results in Table 1 show that the amphiphiles are capable of gelating only aromatic solvents at a concentration less than 6% (w/v) at room temperature (298 K). It is observed that in any given solvent, for example in benzene, the amphiphile **4** has the lowest CGC value among all the amphiphiles. The variation of CGC with hydrocarbon chain lengths (C_n) is shown in Figure 2. The CGC value decreases with increasing C_n value in going from amphiphile **1** to **4**. Interestingly, gelator **5**, in spite of having higher chain length (C_{16}) has CGC value slightly higher than that of **4**. The higher CGC value of **5** in comparison to **4** may be attributed to bending of the hydrocarbon chain. It is well-known that normally up to C_{14} chain length the hydrocarbon tail remains

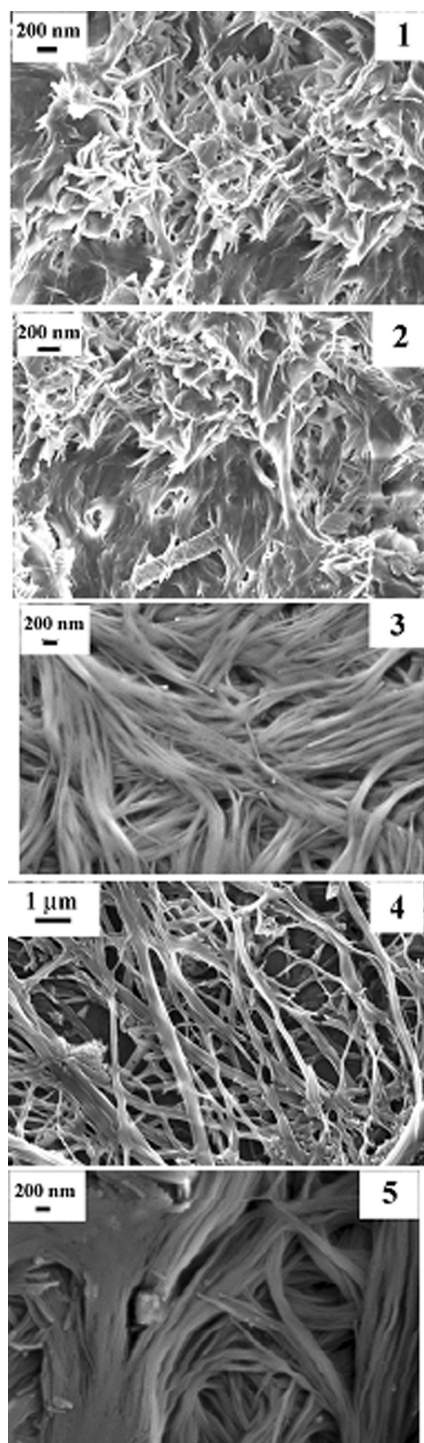


Figure 4. FESEM images of the air-dried organogels of the gelators **1**–**5** in benzene containing 5.45% (w/v) gelator.

straight and then starts to bend with further increase of the number of methylene groups. The bent hydrocarbon tail in the case of gelator **5** may inhibit tight packing in the self-assembled structure thus inhibiting growth of the 1-D aggregates. This is indicated by the melting point of solid gelator **5** (348 K) which is slightly less than that of gelator **4** (352 K).

The data in Table 1 show that for any given gelator the CGC value does not change significantly in going from benzene to nitrobenzene. In order to analyze the solvent effect on gelation ability of a gelator, we correlate the CGC values of **4** and **5** as

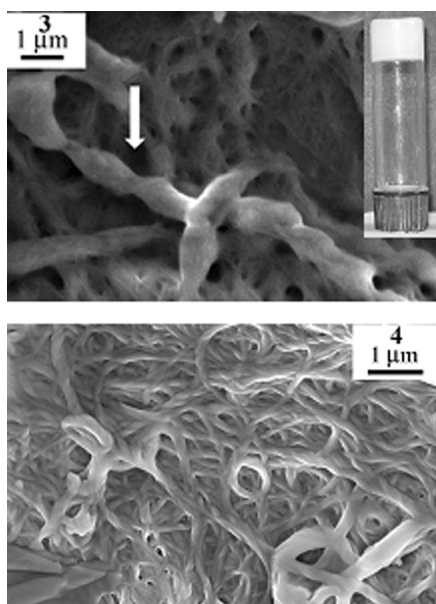


Figure 5. FESEM images of the gels in 80% (v/v) ethanol/water of 3 and 4.

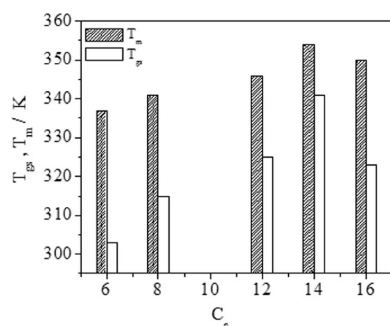


Figure 6. Variation of gel-to-sol transition temperature (T_{gs}) of benzene organogels (0.1 M) and solid melting temperature (T_m) as a function of C_n .

representative gelators with the polarity parameters, such as Kamlet–Taft parameter (π^*) and dielectric constant (ϵ) of different solvents.⁴⁸ The plots of CGC versus ϵ (Figure 3a) for both gelators do not show any correlation, indicating that dielectric constant does not play any significant role in regulating the specific gelator–solvent interactions at the molecular level. This is also confirmed by the CGC values of 3 and 4 in an ethanol/water mixtures (discussed below) which are closely similar to the corresponding value in pure aromatic solvents. We then compared the effect of solvent on CGC in terms of Kamlet–Taft parameters that describe solvents not only in terms generalized polarity parameter (π^*) but also in terms of their hydrogen bond donating (α) and accepting (β) ability. Since the solvents (except chlorobenzene and nitrobenzene) gelled have neither hydrogen bond donating nor accepting ability, CGC values were plotted as a function only π^* parameter (Figure 3b). However, only a weak correlation could be observed for the gelators 4 and 5. Very recently, Feng et al. showed that the gelation behavior of a good LMWG can be predicted by the use of regular solution model and solubility parameter theory.⁴⁹ In order to examine this, we have correlated T_{gs} values of 4 and 5 with Hildebrand solubility parameter (δ).⁵⁰ Again no correlation of gelation ability with

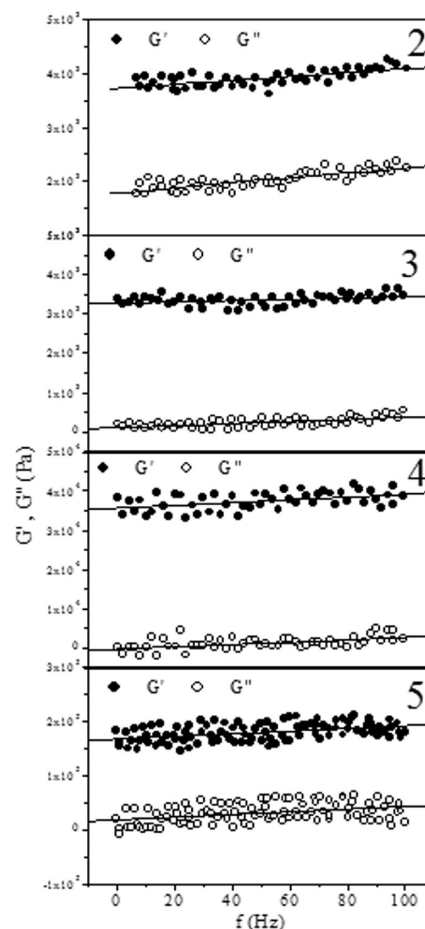


Figure 7. Variation of storage modulus (G') and loss modulus (G'') of benzene gels containing 0.1 M (A) 2, (B) 3, (C) 4, and (D) 5 with frequency (f).

the δ parameter could be observed in the plots shown in Figure 3c.

Gelation of Ethanol/Water Mixtures. The gelation behavior was also investigated in pure water, but the gelators remained insoluble even on heating. This behavior is similar to most surface-active ureas that suffer from poor aqueous solubility because of strong bifurcated intermolecular H-bonding between urea groups of neighboring molecules.⁵¹ On the other hand, they were found to be very soluble in pure ethanol. In ethanol/water mixtures containing low volume percentages of water, these gelators precipitated out when cooled to room temperature. However, it was interesting to observe that the suspension of 3 and 4 in ethanol/water mixtures containing water between 15% and 25% becomes soluble on heating and gels the mixture when cooled to the room temperature. The gels appear opaque. The organogels were observed to be stable at ~ 303 K as long as the condition was kept constant. The CGC values (Table S1, S1) show that best gelation is observed in 20% ethanol/water mixture for both gelators. The gelation ability of 3 and 4 decreases in mixtures having ethanol/water ratio above or below this composition. It is observed that the CGC value of gelators 3 and 4 in 20% ethanol/water mixture is slightly less than that of the organogels in the aromatic solvents. As in the case of organogels, the gelation ability of gelator 4 is higher than that for 3, indicating the role of van der Waals interaction between hydrocarbon chains in the gelation process. The inability of the

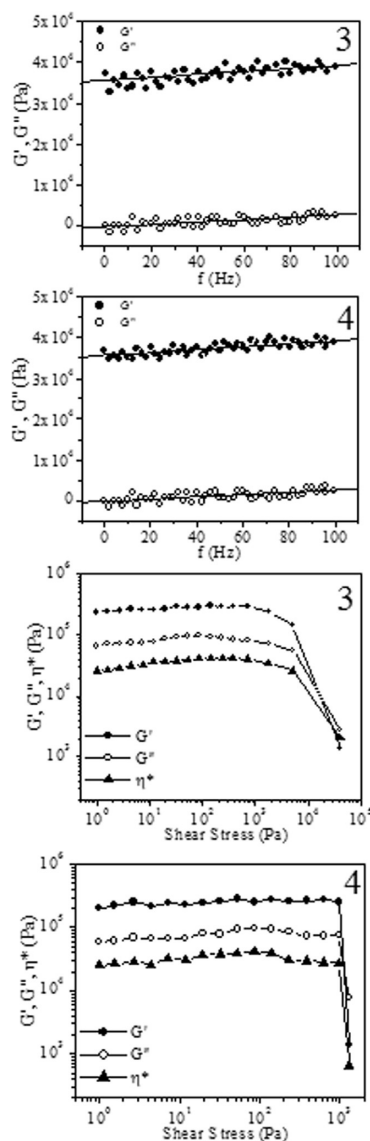


Figure 8. Variation of G' , G'' , and η^* of the 3 and 4 gels (0.1 M) in 80% ethanol/water mixture with frequency (f) and shear stress (σ).

gelator 5 to produce gel in ethanol/water mixture, as discussed earlier, must be a consequence of hydrocarbon chain bending that affects chain packing. Surprisingly, the gelators 3–5 failed to gel methanol/water mixtures. Therefore, it appears that, and as discussed above, perhaps solvent dielectric constant has no significant role in gelation for this class of compounds.

Morphology. The 3-D network structures of the gels are known to immobilize the solvent. The network structures formed in benzene organogels of the gelators 1–5 were confirmed by the FESEM images (Figure 4). The FESEM images clearly reveal intertwined ribbonlike aggregates. However, the aspect ratio of the aggregates seems to be lower in the case of gelators 1 and 2 that have shorter hydrocarbon chain length. This means that the length of hydrocarbon tail is very important for gelation to occur. In other words, van der Waals interactions between hydrocarbon tails are the driving forces for aggregate formation. It is well established that LMWGs usually self-assemble into 1-D fibrillar structures which have a strong tendency to bundle. In the case of gelators 1–5, the 1-D lamellar structures formed through interactions of the hydrocarbon chains either by physical

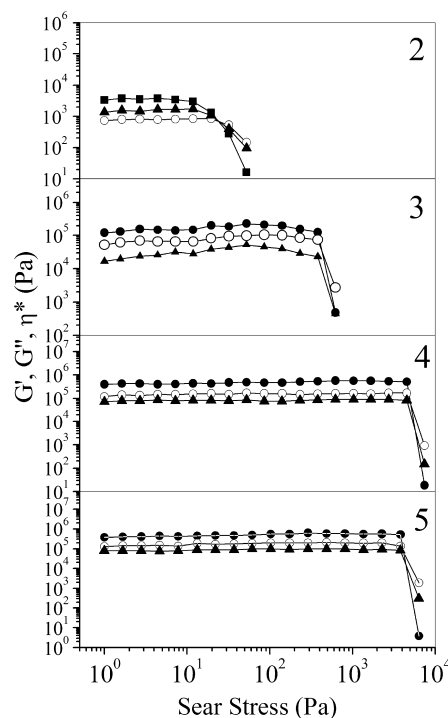


Figure 9. Variation of storage modulus (G'), loss modulus (G''), and complex viscosity (η^*) of benzene gels containing 0.1 M (A) 2, (B) 3, (C) 4, and (D) 5 with shear stress (σ).

entanglement or branching or both form 3-D network structure as shown by the FESEM images.

The microstructures of the organogels 3 and 4 in ethanol/water mixtures are similar to that of the corresponding organogel in benzene. Representative FESEM images of the gels in 80% ethanol/water containing 5.45% (w/v) gelator are shown in Figure 5. It can also be seen that the ribbons appear to be thicker in ethanol/water gel, which can strengthen the 3-D network structure. This is confirmed by the rheological data as discussed below. It is interesting to see some twisting (indicated by arrow) of the ribbons in the micrograph of 3 organogel in 20% ethanol/water mixture. The existence of helical structure in the gel state could not be confirmed by circular dichroism spectra because the gels were optically opaque (see inset, Figure 5). However, it can be speculated that helical structures are formed as a result of gelation.

The existence of lamellar structures is also confirmed by the XRD patterns (Figure S7, SI) of the xerogels of both benzene and ethanol/water mixture organogels, exhibiting periodic reflection peaks. The relative peak position ($q_1:q_2:q_3 \dots = 1:2:3 \dots$) corresponds to 100, 200, and 300 planes. The Bragg scattering pattern suggests that the gelator assembles into an ordered 1-D lamellar structure. The bilayer thickness of the lamella which is equal to the interlayer distance (d) of the 100 plane is 2.93 nm for benzene gel and 2.97 nm for ethanol/water gel of 4. The bilayer thickness is approximately equal to twice the extended molecular length of the hydrophobic tail of the amphiphile.⁵² Thus, the XRD data clearly suggest that the molecular arrangement in the supramolecular assembly is same in both organogels. The probable arrangement of the molecules is presented in Figure S8 of the SI.

Driving Force for Gelation. We have utilized FT-IR spectroscopy to evaluate the interdigitation of the hydrocarbon tails and also the strength of H-bonding interactions,

responsible for the gelation of these compounds. An efficient interdigitation of the hydrocarbon chains in gelator **4** ($\nu \sim 2920$ and 2850 cm^{-1}) as suggested by the sharp peaks corresponding to the $-\text{CH}_2-$ groups (Figure S1, SI). The interdigitation is, however, less in the case of gelator **5**. This can be attributed to chain bending as discussed earlier. The stretching N–H and amide-I bands and the bending amide-II band of **4** ($\nu \sim 3355$, 1630 , and 1578 cm^{-1} , respectively) and **5** (Figure S2, SI; $\nu \sim 3330$, 1645 , and 1550 cm^{-1} , respectively) suggest that NH–CO–NH and NH–CO–S groups are strongly H-bonded because they are red-shifted from the stretching vibrations (1680 – 1650 cm^{-1} for amide-I and carbamoylsulfanyl)⁵³ of the non-hydrogen-bonded molecule. On the other hand, the C=O stretching frequency of the non-hydrogen-bonded –COOH group is about 1725 cm^{-1} . The –COOH headgroup of the gelator molecules in the self-assembly can exist either in the H-bonded acyclic or cyclic dimer forms. Therefore, the FT-IR spectra in the region of –COOH absorptions (Figure S6, SI) were also analyzed. The small peak at 1708 cm^{-1} can be attributed to single in-plane H-bonded acyclic dimer. In order to gain more insights into the molecular arrangements within the fibers and to substantiate the FT-IR data, we have performed concentration dependent and variable temperature ^1H NMR experiments (Figures S9 and S10, SI). It can be seen that, in the gel state, the chemical shift positions of the –NH– proton(s) of the urea and/or sulfamide groups at room temperature are missing, but they appear with the rise of temperature. Also, the peak for –NH– exhibits shift toward high field with the increase in temperature. This means that the –NH– proton(s) of the urea and/or sulfamide groups in the gelator molecule are strongly H-bonded in the self-assembled structure. These data suggest that a combination of three H-bonded amide groups and the van der Waals interactions between hydrocarbon chains strongly reinforce the self-assembly of these organogelators.

Thermal Stability. The thermal stability of the organogels in benzene as well as in ethanol/water mixtures was investigated by measuring gel-to-sol transition temperature (T_{gs}) at a fixed molar concentration (0.1 M). The plot of T_{gs} values of benzene organogels as a function of C_n is shown in Figure 6. It can be observed that the change of T_{gs} values follow the same trend as observed with melting of solid compounds (T_m). That is, T_{gs} initially increases with chain length and then suddenly drops down with further increase. The lower T_{gs} values (303–310 K) in the case of organic solvents suggest low thermal stability of the organogels compared to the gels in ethanol/water mixtures (323–337 K). It is well-known that T_{gs} depends on the thermodynamic driving forces that are responsible for the self-assembly formation. Although the gelator has strong H-bonding urea and sulfamide linkages, it appears that van der Waals and solvophobic interactions of the alkyl chains are the major driving forces for gelation. If H-bonding interaction had a major role, then gelation would not occur in ethanol/water mixture that interferes H-bonding. Low melting points ($\sim 354 \text{ K}$) of the solid gelators also suggest weaker interactions among gelator molecules in the solid state. The higher thermal stability of the gels in ethanol/water mixture is therefore due to stronger solvophobic interaction of the alkyl chains.

Mechanical Strength of the Organogels. It is essential to know the mechanical properties of the organogels because mechanical strength or elastic behaviors of the organogels are directly linked to their applications. Thus we used oscillatory

rheology to assess the elasticity of the organogels made of the amphiphilic gelators. The mechanical strength of a gel which is measured by the storage modulus (G') and loss modulus (G'') is dependent on gelator concentration. Therefore, to compare the viscoelastic property of the gels, rheology measurements were performed with a fixed (0.1 M) gelator concentration in benzene. The frequency sweep (Figure 7) measurements indicate that G' and G'' values of the organogels are independent of frequency (f) and at any given frequency, the G' is greater than G'' , suggesting that the organogels behave like solids. The organogel formed by **1** showed rheological behavior with the magnitude of the G' very close to that of G'' (data not shown), suggesting weak mechanical strength. The absence of a stable value during frequency sweep measurement is consistent with the feature of a weak organogel. The results in Figure 7 clearly show that at a given frequency (65 Hz) G'/G'' value decreases in the order $4 > 3 > 2$. In other words, elasticity of the organogels increases with the increase of hydrocarbon chain length. It should also be noted that the G' value of the organogel **5** is slightly less than that of **4**, indicating decrease of mechanical strength. The elastic nature of the **3** and **4** organogels in 80% ethanol/water mixture could also be observed as shown by the frequency sweep measurements in Figure 8.

The mechanical strength of the benzene organogels was further estimated by the amplitude sweep measurements. Figure 9 shows the plots of G' , G'' , and complex viscosity (η^*) versus applied stress (σ) at a constant frequency of 1 Hz. It can be observed that, above a critical stress value referred to as yield stress (σ_y), G' , G'' , and η^* of the benzene organogels of **2**–**5** abruptly fall to a very low value, indicating flow of the gel. The σ_y values of the benzene gels increases in the order **2** (12 Pa) < **3** (388 Pa) < **4** (4706 Pa). However, the σ_y value of the benzene gel of **5** (3756 Pa) was observed to be less than that of **4**. This means that up to a certain limit the mechanical strength of the organogels increases with increasing hydrocarbon chain length and then it falls down. This trend is very similar to what is observed with CGC, T_{gs} , and T_m values of the organogels as discussed above. This means that mechanical strength of the gels is dependent on the intermolecular interactions involved in the gelation process. The stress amplitude sweep of the ethanol/water organogels are shown in Figure 8. The higher values of σ_y of **3** (950 Pa) and **4** (5041 Pa) organogels in 80% ethanol/water mixture compared to the σ_y value of the corresponding benzene gel suggest higher stability of the ethanol/water gel than the benzene gel. The higher stability toward shear stress of the ethanol/water gel compared to benzene gel can be attributed to the morphological difference as discussed above. Indeed FESEM images in Figure 5 show that the ribbons of high aspect ratio are thicker, twisted and more entangled in the ethanol/water mixture gel.

CONCLUSIONS

In summary, we have developed L-cysteine based LMWGs **1**–**5** of which **2**–**5** efficiently gelate only aromatic solvents at relatively low concentrations (CGC $\leq 6\%$ w/v). Among the gelators, **3** and **4** are ambidextrous and also gelled ethanol/water mixtures at a slightly lower concentration than in benzene. The organogels in benzene as well as in ethanol/water mixtures show 3-D networks of ribbonlike structures. The ethanol/water gels of both **3** and **4** also exhibit helical ribbonlike chiral aggregates. The gelation ability of the gelators increases with the increase of hydrocarbon chain length. The

van der Waals as well as H-bonding interactions are the driving forces for the 1-D aggregate formation. The organogels were found to be thermoreversible. The thermal stability increased with the increase of hydrocarbon chain length, that is with the increase of van der Waals interactions. But the stability increases up to C14 chain length and then it dropped down due to bending of the hydrocarbon chain which causes chain packing less tight. A similar trend was also observed with the mechanical strength of the benzene and ethanol/water organogels. Thus, mechanical strength of the organogels is also dependent on the molecular interactions that are responsible for gelation. The mechanical strength of the gel in 80% ethanol/water mixture was observed to be greater than that in benzene. Also the gels in ethanol/water mixtures have melting temperatures higher than the physiological temperature. Thus, they may have potential application in transdermal drug delivery.^{54,55}

■ ASSOCIATED CONTENT

■ Supporting Information

Details of synthesis and chemical identification of structures by ¹H NMR, ¹³C NMR, FT-IR spectra, table for gelation properties and critical gelation concentration of the gelators **3** and **4** in ethanol/water mixtures, XRD patterns of the gel cast film of the gelators in benzene and in ethanol/water mixture, packing of gelator molecules in the bilayer assembly, concentration-dependent and variable temperature ¹H NMR spectra in benzene-*d*₆. This material is available free of charge via the Internet at <http://pubs.acs.org>.

■ AUTHOR INFORMATION

Corresponding Author

*Fax: (+) 91-3222-255303 E-mail: joydey@chem.iitkgp.ernet.in.

Notes

The authors declare no competing financial interest.

■ ACKNOWLEDGMENTS

The authors gratefully acknowledge Indian Institute of Technology Kharagpur for financial support of this work. We thank Mr Kiran Patruni for assistance with the rheology measurements.

■ REFERENCES

- (1) Feringa, B. L.; van Esch, J.; Feringa, B. L.; van Esch, J. Entrapment and Release of Quinoline Derivatives Using a Hydrogel of a Low Molecular Weight Gelator. *J. Controlled Release* **2004**, *97*, 241–248.
- (2) Ishi-I, T.; Shinkai, S. Dye-Based Organogels: Stimuli-Responsive Soft Materials Based on One-Dimensional Self-Assembling Aromatic Dyes. *Top. Curr. Chem.* **2005**, *258*, 119–160.
- (3) Sreenivasachary, N.; Lehn, J. M. Gelation-Driven Component Selection in the Generation of Constitutional Dynamic Hydrogels Based on Guanine-Quartet Formation. *Proc. Natl. Acad. Sci. U.S.A.* **2005**, *102*, 5938–5943.
- (4) Friggeri, A.; Chitkara, D.; Shikanov, A.; Kumar, N.; Domb, A. J. Biodegradable Injectable In Situ Depot-Forming Drug Delivery Systems. *Macromol. Biosci.* **2006**, *6*, 977–990.
- (5) Vemula, P.; Li, J.; John, G. Enzyme Catalysis: Tool to Make and Break Amygdalin Hydrogelators from Renewable Resources: A Delivery Model for Hydrophobic Drugs. *J. Am. Chem. Soc.* **2006**, *128*, 8932–8938.
- (6) Ellis-Behnke, R. G.; Liang, Y. X.; You, S.-W.; Tay, D. K. C.; Zhang, S.; So, K.-F.; Schneider, G. E. Nano Neuro Knitting: Peptide

Nanofiber Scaffold for Brain Repair and Axon Regeneration With Functional Return of Vision. *Proc. Natl. Acad. Sci. U.S.A.* **2006**, *103*, 5054–5059.

- (7) Khatua, D.; Maiti, R.; Dey, J. A Supramolecular Hydrogel That Responds to Biologically Relevant Stimuli. *Chem. Commun.* **2006**, 4903–4905.

- (8) Yang, Z.; Liang, G.; Yang, Z. M.; Ho, P. L.; Liang, G. L.; Chow, K. H.; Wang, Q. G.; Cao, Y.; Guo, Z. H.; Xu, B. Using β -Lactamase to Trigger Supramolecular Hydrogelation. *J. Am. Chem. Soc.* **2007**, *129*, 266–267.

- (9) Shi, N.; Dong, H.; Yin, G.; Xu, Z.; Li, S. A Smart Supramolecular Hydrogel Exhibiting pH-Modulated Viscoelastic Properties. *Adv. Funct. Mater.* **2007**, *17*, 1837–1843.

- (10) Shome, A.; Debnath, S.; Das, P. K. Head Group Modulated pH-Responsive Hydrogel of Amino Acid-Based Amphiphiles: Entrapment and Release of Cytochrome *c* and Vitamin B₁₂. *Langmuir* **2008**, *24*, 4280–4288.

- (11) Yang, Z. M.; Liang, G. L.; Xu, B. Enzymatic Hydrogelation of Small Molecules. *Acc. Chem. Res.* **2008**, *41*, 315–326.

- (12) Wada, A.; Tamaru, S.; Ikeda, M.; Hamachi, I. MCM–Enzyme–Supramolecular Hydrogel Hybrid as a Fluorescence Sensing Material for Poly-anions of Biological Significance. *J. Am. Chem. Soc.* **2009**, *131*, 5321–5330.

- (13) Komatsu, H.; Matsumoto, S.; Tamaru, S.; Kaneko, K.; Ikeda, M.; Hamachi, I. Supramolecular Hydrogel Exhibiting Four Basic Logic Gate Functions To Fine-Tune Substance Release. *J. Am. Chem. Soc.* **2009**, *131*, 5580–5585.

- (14) Vemula, P. K.; Cruikshank, G.; Karp, J. M.; John, G. Self-Assembled Prodrugs: An Enzymatically Triggered Drug-Delivery Platform. *Biomaterials* **2009**, *30*, 383–393.

- (15) Terech, P.; Weiss, R. G. Low Molecular Mass Gelators of Organic Liquids and the Properties of Their Gels. *Chem. Rev.* **1997**, *97*, 3133–3160.

- (16) Estroff, L. A.; Hamilton, A. D. Water Gelation by Small Organic Molecules. *Chem. Rev.* **2004**, *104*, 1201–1218.

- (17) Sangeetha, N. M.; Maitra, U. Supramolecular Gels: Functions and Uses. *Chem. Soc. Rev.* **2005**, *34*, 821–836.

- (18) *Molecular Gels: Materials with Self-Assembled Fibrillar Networks*; Weiss, R. G., Terech, P., Eds.; Springer: Dordrecht, 2006.

- (19) George, M.; Weiss, R. G. Molecular Organogels. Soft Matter Comprised of Low-Molecular-Mass Organic Gelators and Organic Liquids. *Acc. Chem. Res.* **2006**, *39*, 489–497.

- (20) Estroff, L. A.; Leiserowitz, L.; Addadi, L.; Weiner, S.; Hamilton, A. D. Characterization of an Organic Hydrogel: A Cryo-Transmission Electron Microscopy and X-ray Diffraction Study. *Adv. Mater.* **2003**, *15*, 38–42.

- (21) Smith, D. K. Lost in translation? Chirality Effects in the Self-assembly of Nanostructured Gel-Phase Materials. *Chem. Soc. Rev.* **2009**, *38*, 684–694.

- (22) Hanabusa, K.; Shimura, K.; Hirose, K.; Kimura, M.; Shirai, H. Formation of Organogels by Intermolecular Hydrogen Bonding Between Ureylene Segment. *Chem. Lett.* **1996**, 885–886.

- (23) Hanabusa, K.; Tanaka, R.; Suzuki, M.; Kimura, M.; Shirai, H. Excellent Gelators for Organic Fluids: Simple Bolaform Amides Derived from Amino Acids. *Adv. Mater.* **1997**, *9*, 1095–1097.

- (24) Wang, G.; Hamilton, A. D. Low Molecular Weight Organogelators for Water. *Chem. Commun.* **2003**, 310–311.

- (25) Suzuki, M.; Sato, T.; Shirai, H.; Hanabusa, K. Powerful Low-Molecular-Weight Gelators Based on L-valine and L-isoleucine with Various Terminal Groups. *New J. Chem.* **2006**, *30*, 1184–1191.

- (26) Hardy, J. G.; Hirst, A. R.; Ashworth, I.; Brennan, C.; Smith, D. K. Exploring Molecular Recognition Pathways within a Family of Gelators with Different Hydrogen Bonding Motifs. *Tetrahedron* **2007**, *63*, 7397–7406.

- (27) Bhattacharya, S.; Ghosh, Y. K. Chemical Regeneration of Human Tooth Enamel Under Near-Physiological Conditions. *Chem. Commun.* **2009**, 5892–5894.

- (28) Steed, J. W. Anion Tuning of the Rheology, Morphology and Gelation of a Low Molecular Weight Salt Hydrogelator. *Soft Matter* **2011**, *7*, 75–84.
- (29) Patra, T.; Pal, A.; Dey, J. Birefringent Physical Gels of *N*-(4-*n*-alkoxybenzoyl)-L-alanine Amphiphiles in Organic Solvents: The Role of Hydrogen-Bonding. *J. Colloid Interface Sci.* **2010**, *344*, 10–20.
- (30) Khatua, D.; Dey, J. Spontaneous Formation of Gel Emulsions in Organic Solvents and Commercial Fuels Induced by a Novel Class of Amino Acid Derivatized Surfactants. *Langmuir* **2005**, *21*, 109–114.
- (31) MacDonald, J. C.; Whitesides, G. M. Solid-State Structures of Hydrogen-Bonded Tapes Based on Cyclic Secondary Diamides. *Chem. Rev.* **1994**, *94*, 2383–2420.
- (32) Esch, J. V.; DeFeyter, S.; Kellogg, R. M.; DeSchryver, S.; Feringa, B. L. Self-Assembly of Bisurea Compounds in Organic Solvents and on Solid Substrates. *Chem.—Eur. J.* **1997**, *3*, 1238–1243.
- (33) Esch, J. V.; Schoonbeek, F.; de Loos, M.; Kooijman, H.; Spek, A. L.; Kellogg, R. M.; Feringa, B. L. Cyclic Bis-Urea Compounds as Gelators for Organic Solvents. *Chem.—Eur. J.* **1999**, *5*, 937–950.
- (34) de Loos, M.; Esch, J. V.; Kellogg, R. M.; Feringa, B. L. Chiral Recognition in Bis-Urea-Based Aggregates and Organogels through Cooperative Interactions. *Angew. Chem., Int. Ed.* **2001**, *40*, 613–616.
- (35) Seki, T.; Fukuchi, T.; Ichimura, K. Role of Hydrogen Bonding in Azobenzene-Urea Assemblies. The Packing State and Photoresponse Behaviour in Langmuir Monolayers. *Langmuir* **2002**, *18*, 5462–5467.
- (36) Kobayashi, T.; Seki, T. Odd – Even effects in Azobenzene-Urea Amphiphile Assemblies. *Langmuir* **2003**, *19*, 9297–9304.
- (37) Dreger, K.; Zou, B.; Mu, Z.; Galla, J. H.; Chi, L.; Fuchs, H.; Schaefer, H. J. Synthesis and Surface Properties of New Urea and Amides at Different Interfaces. *Langmuir* **2006**, *22*, 1619–1625.
- (38) Yoshimura, T.; Sakato, A.; Tsuchiya, K.; Ohkubo, H.; Sakai, H.; Abe, M.; Esumi, K. Adsorption and Aggregation Properties of Amino Acid-based *N*-alkyl Cystein Monomeric and *N,N'*-dialkyl Cystein Gemini Surfactants. *J. Colloid Interface Sci.* **2007**, *308*, 466–473.
- (39) Fan, H.; Han, F.; Liu, Z.; Qin, L.; Li, Z.; Liang, D.; Ke, F.; Huang, J.; Fu, H. Active Control of Surface Properties and Aggregation Behaviour in Amino Acid-Based Gemini Surfactant Systems. *J. Colloid Interface Sci.* **2008**, *321*, 227–234.
- (40) George, M.; Tan, G.; John, V. T.; Weiss, R. G. Urea and Thiourea Derivatives as Low Molecular-Mass Organogelators. *Chem.—Eur. J.* **2005**, *11*, 3243–3254.
- (41) Pal, A.; Dey, J. Water-Induced Physical Gelation of Organic Solvents by *N*-(*n*-alkylcarbonyl)-L-alanine Amphiphiles. *Langmuir* **2011**, *27*, 3401–3408.
- (42) Maeda, H. Anion-Responsive Supramolecular Gels. *Chem.—Eur. J.* **2008**, *14*, 11274–11282.
- (43) Lloyd, G. O.; Steed, J. W. Anion-Tuning of Supramolecular Gel Properties. *Nat. Chem.* **2009**, *1*, 437–442.
- (44) Ho, S. E.; Ide, N.; Lau, B. H. S-Allyl Cysteine Reduces Oxidant Load in Cells Involved in the Atherogenic Process. *Phytomedicine* **2001**, *8*, 39–46.
- (45) Menger, F. M.; Caran, K. L. Anatomy of a Gel. Amino Acid Derivatives That Rigidify Water at Submillimolar Concentrations. *J. Am. Chem. Soc.* **2000**, *122*, 11679–11691.
- (46) Menger, F. M.; Zhang, H.; Caran, K. L.; Seredyuk, V. A.; Apkarian, R. P. Gemini-Induced Columnar Jointing in Vitreous Ice. Cryo-HRSEM as a Tool for Discovering New Colloidal Morphologies. *J. Am. Chem. Soc.* **2002**, *124*, 1140–1141.
- (47) Ilyin, S.; Roumyantseva, T.; Spiridonova, V.; Semakov, A.; Frenkin, E.; Malkin, A.; Kulichikhin, V. Gels of Cysteine/Ag-Based Dilute Colloid Systems and Their Rheological Properties. *Soft Matter* **2011**, *7*, 9090–9103.
- (48) Kamlet, M. J.; Abboud, J. L. M.; Abraham, M. H.; Taft, R. W. Linear Solvation Energy Relationships. 23. A Comprehensive Collection of the Solvatochromic Parameters, π , α , and β , and Some Methods for Simplifying the Generalized Solvatochromic Equation. *J. Org. Chem.* **1983**, *48*, 2877–2887.
- (49) Feng, L.; Cavicchi, K. A. Investigation of the relationship between the thermodynamic phase behavior and gelation behavior of a series of tripodal trisamide compounds. *Soft Matter* **2012**, *8*, 6483–6492.
- (50) Barton, A. F. M. Solubility Parameters. *Chem. Rev.* **1975**, *75*, 731–753.
- (51) Coe, S.; Kane, J. J.; Nguyen, T. L.; Toledo, L. M.; Winger, E.; Fowler, F. W.; Lauher, J. W. Molecular Symmetry and the Design of Molecular Solids: The Oxalamide Functionality as a Persistent Hydrogen Bonding Unit. *J. Am. Chem. Soc.* **1997**, *119*, 86–93.
- (52) The length of the hydrophobic chain which excludes NH–CO–NH or NH–CO–S linkage was calculated using MM2 program of CS Chem3D Std software.
- (53) Fernández, G.; García, F.; Aparicio, F.; Matesanz, E.; Sánchez, L. Two-Dimensional Self-Organization of Rectangular OPE Amphiphiles into Microcrystalline Lamellae. *Chem. Commun.* **2009**, 7155.
- (54) Al-Saidan, S. M.; Krishnaiah, Y. S. R.; Chandrasekhar, D. V.; Lalla, J. K.; Rama, B.; Jayaram, B.; Bhaskar, P. Formulation of an HPMC Gel Drug Reservoir System with Ethanol–Water as a Solvent System and Limonene as a Penetration Enhancer for Enhancing in vitro Transdermal Delivery of Nicorandil. *Skin Pharmacol. Physiol.* **2004**, *17*, 310–320.
- (55) Krishnaiah, Y. S.; Bhaskar, P.; Satyanaraya, V. Penetration Enhancing Effect of Ethanol–Water Solvent System and Ethanolic Solution of Carvone on Transdermal Permeability of Nimodipine from HPMC Gel Across Rat Abdominal Skin. *Skin Pharm. Dev. Technol.* **2004**, *9*, 63–74.